

The semi-constrained NMSSM in light of muon $g-2$, LHC, and dark matter constraints^{*}

Kun Wang¹ Fei Wang² Jingya Zhu^{1;1)} Quanlin Jie¹¹ Center for Theoretical Physics, School of Physics and Technology, Wuhan University, Wuhan 430072, China² School of Physics, Zhengzhou University, Zhengzhou 450000, China

Abstract: The semi-constrained NMSSM (scNMSSM) extends the MSSM by a singlet field, and requires unification of the soft SUSY breaking terms in the squark and slepton sectors, while it allows that in the Higgs sector to be different. We try to interpret the muon $g-2$ in the scNMSSM, under the constraints of 125 GeV Higgs data, B physics, searches for low and high mass resonances, searches for SUSY particles at the LHC, dark matter relic density by WMAP/Planck, and direct searches for dark matter by LUX, XENON1T, and PandaX-II. We find that under the above constraints, the scNMSSM can still (i) satisfy muon $g-2$ at 1σ level, with a light muon sneutrino and light chargino; (ii) predict a highly-singlet-dominated 95 GeV Higgs, with a diphoton rate as hinted at by CMS data, because of a light higgsino-like chargino and moderate λ ; (iii) get low fine tuning from the GUT scale with small $\mu_{\text{eff}}, M_0, M_{1/2},$ and A_0 , with a lighter stop mass which can be as low as about 500 GeV, which can be further checked in future studies with search results from the 13 TeV LHC; (iv) have the lightest neutralino be singlino-dominated or higgsino-dominated, while the bino and wino are heavier because of high gluino bounds at the LHC and universal gaugino conditions at the GUT scale; (v) satisfy all the above constraints, although it is not easy for the lightest neutralino, as the only dark matter candidate, to get enough relic density. Several ways to increase relic density are discussed.

Keywords: NMSSM, supersymmetry phenomenology, dark matter**PACS:** 11.30 Pb **DOI:** 10.1088/1674-1137/42/10/103109

1 Introduction

In July 2012, the Higgs boson was discovered at the LHC [1, 2], and searching for physics beyond the Standard Model (SM) has now become the main objective in high energy physics. Supersymmetry (SUSY) is one of the most popular theories for new physics. As the simplest SUSY model, the minimal supergravity model (mSUGRA) has attracted a lot of attention from both theorists and experimentalists. However, it cannot predict a 125 GeV SM-like Higgs when considering all the constraints, including muon $g-2$ at 2σ level, and dark matter [3, 4]. When we give up uniform parameters at the grand unification (GUT) scale, the MSSM can satisfy all the constraints well, but there is a problem with fine-tuning [4].

After the Higgs boson was discovered, it became necessary to ask whether there is a second Higgs-like particle. Searches at LEP, the Tevatron, and the LHC have

excluded a lighter SM-like Higgs, while a lighter second Higgs with rates lower than the SM-like one could still be possible. Recently, the CMS collaboration presented their searches for low-mass new resonances decaying to two photons. For both the 8 TeV and 13 TeV dataset, a small excess around 95 GeV was hinted at, with approximately 2.8σ local (1.3σ global) significance for a hypothetical mass of 95.3 GeV in combined analysis [5]. This result has been interpreted or discussed in several papers [6]. The MSSM cannot predict such a lighter second Higgs together with a 125 GeV SM-like Higgs under other constraints like the muon $g-2$ and dark matter [4].

The next-to-minimal supersymmetric Standard Model (NMSSM) has more freedom to predict a SM-like 125 GeV Higgs, under all the constraints and with low fine-tuning [4]. At the same time, it can also predict a lighter second Higgs with rates lower than the SM-like one [7, 8]. Since simple models are usually more favoured, the fully constrained NMSSM (cNMSSM) [9–

Received 11 June 2018, Published online 12 September 2018

^{*} Supported by National Natural Science Foundation of China (NNSFC) (11605123, 11675147, 11547103, 11547310), the Innovation Talent project of Henan Province (15HASTIT017), and the Young Core Instructor Foundation of Henan Education Department. J. Z. also thanks the support of the China Scholarship Council (CSC) (201706275160) while at the University of Chicago as a visiting scholar, and the U.S. National Science Foundation (NSF) (PHY-0855561) while at Michigan State University from 2014-2015.

1) E-mail: zhujy@itp.ac.cn

©2018 Chinese Physical Society and the Institute of High Energy Physics of the Chinese Academy of Sciences and the Institute of Modern Physics of the Chinese Academy of Sciences and IOP Publishing Ltd

11] and the semi-constrained NMSSM (scNMSSM) are also being studied [12, 13]. For the full cNMSSM, with all soft SUSY breaking terms unified at the GUT scale, including $M_{H_u} = M_{H_d} = M_S = M_0$, there should be only four continuous parameters, the same as mSUGRA. While in many studies of the cNMSSM [9–11], there is an additional parameter λ , for a singlet scalar M_S does not in fact need to be unified. Such an issue was also pointed out in Ref. [14]. In the 5-parameter and 4-parameter cNMSSM, the SM-like Higgs cannot get to 125 GeV under all the constraints including muon g-2 [9, 11]. The scNMSSM is also called the non-universal Higgs mass (NUHM) version of the NMSSM, for it allows the soft SUSY breaking terms in the Higgs sector to be different. In Ref. [9], the parameter λ is always less than 0.1, so the results in Higgs sector may not be much different from the NUHM version of MSSM, e.g., the 125 GeV SM-like Higgs is always the lightest Higgs. In Refs. [12, 13], the muon g-2 constraint is set aside. In this paper, we consider all the constraints, including muon g-2, and also require a lighter Higgs with rates constrained by LEP, Tevatron, and LHC searches. For the dark matter relic density, we only apply the upper bound [8], considering that there may be other sources of dark matter [15]. We focus on the muon g-2, its relation to model parameters, SUSY particle masses, and other constraints like the dark matter relic density.

This paper is organized as follows. First, we briefly introduce the NMSSM and scNMSSM in Section 2. In Section 3, we discuss the constraints on the model, present our numerical results and have some discussion. Finally, we draw our conclusions in Section 4.

2 The NMSSM and scNMSSM

In the NMSSM, the Higgs sector consists of two complex doublet superfields \hat{H}_u and \hat{H}_d , and one complex singlet superfield \hat{S} . Then the superpotential of the NMSSM with Z_3 symmetry is given by [16]

$$W_{\text{NMSSM}} = \lambda \hat{S} \hat{H}_u \cdot \hat{H}_d + \frac{\kappa}{3} \hat{S}^3 + W_F, \quad (1)$$

where W_F is the superpotential of the MSSM without the μ -term, which is the Yukawa couplings of \hat{H}_u and \hat{H}_d to the quark and lepton superfields [17]. At electroweak symmetry breaking, the Higgs fields \hat{H}_u , \hat{H}_d and \hat{S} get their vacuum expectation values (VEVs) v_u , v_d and v_s respectively, with $\tan\beta \equiv v_u/v_d$. Then their scalar component fields can be written as

$$H_u = \begin{pmatrix} H_u^+ \\ v_u + \frac{\phi_u + i\varphi_u}{\sqrt{2}} \end{pmatrix}, \quad H_d = \begin{pmatrix} v_d + \frac{\phi_d + i\varphi_d}{\sqrt{2}} \\ H_d^- \end{pmatrix}, \quad (2)$$

$$S = v_s + \frac{\phi_s + i\varphi_s}{\sqrt{2}},$$

where H_i^+ , ϕ_i and φ_i ($i = u, d$) represent the charged, neutral CP-even and neutral CP-odd component fields respectively. So the first term in W_{NMSSM} generates an effective μ -term,

$$\mu_{\text{eff}} = \lambda v_s. \quad (3)$$

With the superpotential, we can get the so-called ‘F-term’ of the Lagrangian [16],

$$-\mathcal{L}_F = \sum_i \left| \frac{\delta W_{\text{NMSSM}}}{\delta \hat{\Phi}_i} \right|^2, \quad (4)$$

where $\hat{\Phi}_i$ can be any chiral superfield in the superpotential.

Since the singlet field is not included, the D-term is the same as in the MSSM,

$$-\mathcal{L}_D = \frac{1}{2} g_2^2 (|H_u|^2 |H_d|^2 - |H_u \cdot H_d|^2) + \frac{1}{8} (g_1^2 + g_2^2) (|H_u|^2 - |H_d|^2)^2. \quad (5)$$

The soft breaking terms in the NMSSM have 4 main parts. In the Higgs sector, the soft breaking terms are given by

$$-\mathcal{L}_{\text{Higgs}} = M_{H_u}^2 |H_u|^2 + M_{H_d}^2 |H_d|^2 + M_S^2 |S|^2 + \left(\lambda A_\lambda S H_u \cdot H_d + \frac{1}{3} \kappa A_\kappa S^3 + \text{h.c.} \right), \quad (6)$$

where M_{H_u} , M_{H_d} , M_S , A_λ and A_κ are soft breaking parameters. In the mass terms of squarks $\{\tilde{q}_i \equiv (\tilde{u}_{iL}, \tilde{d}_{iL}), \tilde{u}_i^c, \tilde{d}_i^c\}$ and sleptons $\{\tilde{\ell}_i \equiv (\tilde{\nu}_{iL}, \tilde{e}_{iL}), \tilde{e}_i^c\}$ ($i = 1, 2, 3$ refers to generation):

$$-\mathcal{L}_0 = M_{\tilde{q}_i}^2 |\tilde{q}_i|^2 + M_{\tilde{u}_i^c}^2 |\tilde{u}_i^c|^2 + M_{\tilde{d}_i^c}^2 |\tilde{d}_i^c|^2 + M_{\tilde{\ell}_i}^2 |\tilde{\ell}_i|^2 + M_{\tilde{e}_i^c}^2 |\tilde{e}_i^c|^2. \quad (7)$$

In the mass terms of the gauginos \tilde{B} (bino), \tilde{W}^a (winos) and \tilde{G}^a (gluinos):

$$-\mathcal{L}_{1/2} = \frac{1}{2} \left[M_1 \tilde{B} \tilde{B} + M_2 \sum_{a=1}^3 \tilde{W}^a \tilde{W}_a + M_3 \sum_{a=1}^8 \tilde{G}^a \tilde{G}_a \right] + \text{h.c.} \quad (8)$$

In the trilinear interactions between the third generation squarks or sleptons and the Higgs field (the Yukawa coupling of the first two generations can be neglected):

$$-\mathcal{L}_3 = \left(h_t A_t Q \cdot H_u \tilde{u}_3^c + h_b A_b H_d \cdot Q \tilde{d}_3^c + h_\tau A_\tau H_d \cdot L \tilde{e}_3^c \right) + \text{h.c.} \quad (9)$$

Higgs sector: In order to present the mass matrices of the Higgs fields in a physical way, we rotate the Higgs fields by [18]:

$$H_1 = \cos\beta H_u - \epsilon \sin\beta H_d^*, \quad H_2 = \sin\beta H_u + \epsilon \cos\beta H_d^*, \quad H_3 = S, \quad (10)$$

where $\epsilon_{12} = -\epsilon_{21} = 1$ and $\epsilon_{11} = \epsilon_{22} = 0$. With this rotation,

$H_i (i=1,2,3)$ are given by

$$\begin{aligned} H_1 &= \begin{pmatrix} H^+ \\ \frac{S_1 + iP_1}{\sqrt{2}} \end{pmatrix}, \\ H_2 &= \begin{pmatrix} G^+ \\ v + \frac{S_2 + iG^0}{\sqrt{2}} \end{pmatrix}, \\ H_3 &= v_s + \frac{1}{\sqrt{2}}(S_3 + iP_2), \end{aligned} \quad (11)$$

where G^+ and G^0 are Goldstone bosons eaten by W^+ and Z respectively, and $v = \sqrt{v_u^2 + v_d^2} = 174$ GeV is the VEV of the Higgs field in the SM. Thus the field H_2 is the SM Higgs field.

In the CP-conserving NMSSM, the field S_1 , S_2 and S_3 mix to form the three physical CP-even Higgs bosons $h_i (i=1,2,3)$, and the fields P_1 and P_2 mix to form the two physical CP-odd Higgs bosons $a_i (i=1,2)$.

In the basis $\{S_1, S_2, S_3\}$, the elements of the corresponding mass matrix are given by [18]:

$$\begin{aligned} M_{11}^2 &= M_A^2 + (m_Z^2 - \lambda^2 v^2) \sin^2 2\beta, \\ M_{12}^2 &= -\frac{1}{2}(m_Z^2 - \lambda^2 v^2) \sin 4\beta, \\ M_{13}^2 &= -\left(\frac{M_A^2}{2\mu/\sin 2\beta} + \kappa v_s\right) \lambda v \cos 2\beta, \\ M_{22}^2 &= m_Z^2 \cos^2 2\beta + \lambda^2 v^2 \sin^2 2\beta, \\ M_{23}^2 &= 2\lambda\mu v \left[1 - \left(\frac{M_A}{2\mu/\sin 2\beta}\right)^2 - \frac{\kappa}{2\lambda} \sin 2\beta\right], \\ M_{33}^2 &= \frac{1}{4}\lambda^2 v^2 \left(\frac{M_A}{\mu/\sin 2\beta}\right)^2 + \kappa v_s A_\kappa + 4(\kappa v_s)^2 \\ &\quad - \frac{1}{2}\lambda\kappa v^2 \sin 2\beta. \end{aligned} \quad (12)$$

where M_A is the mass scale of the doublet field H_1 , and it is given by

$$M_A^2 = \frac{2\mu}{\sin 2\beta} (A_\lambda + \kappa v_s). \quad (13)$$

The mass matrix in Eq.(12) can be diagonalized by an orthogonal matrix $[S_{ij}]$. We can get the mass eigenstates of CP-even states h_i as

$$h_i = \sum_{j=1}^3 S_{ij} S_j, \quad (14)$$

where S_{ij} are the coefficients of S_j in the mass eigenstate h_i , which satisfy $|S_{i1}|^2 + |S_{i2}|^2 + |S_{i3}|^2 = 1$, and we assume that $m_{h_1} < m_{h_2} < m_{h_3}$. In this work, we regard h_2 as the 125 GeV SM-like Higgs boson, thus $|S_{23}|^2$ is the singlet component in h_2 , and $|S_{23}|^2 < 0.5$.

Neutralino sector: In the NMSSM there are five neutralinos (χ_i^0), which are mixtures of bino (\tilde{B}), wino (\tilde{W}^0), higgsino (\tilde{H}_u, \tilde{H}_d) and singlino (\tilde{S}):

$$\begin{pmatrix} \chi_1^0 \\ \chi_2^0 \\ \chi_3^0 \\ \chi_4^0 \\ \chi_5^0 \end{pmatrix} = N_{ij} \begin{pmatrix} \tilde{B} \\ \tilde{W}^0 \\ \tilde{H}_u \\ \tilde{H}_d \\ \tilde{S} \end{pmatrix}. \quad (15)$$

We assume that the lightest neutralino is the lightest SUSY particle (LSP) and makes up dark matter.

In the basis $\{\tilde{B}, \tilde{W}^0, \tilde{H}_u, \tilde{H}_d, \tilde{S}\}$, the tree-level neutralino mass matrix takes the form [16, 19]

$$M_{\tilde{\chi}^0} = \begin{pmatrix} M_1 & 0 & \frac{g_1 v_u}{\sqrt{2}} & -\frac{g_1 v_d}{\sqrt{2}} & 0 \\ 0 & M_2 & -\frac{g_2 v_u}{\sqrt{2}} & \frac{g_2 v_d}{\sqrt{2}} & 0 \\ \frac{g_1 v_u}{\sqrt{2}} & -\frac{g_2 v_u}{\sqrt{2}} & 0 & -\mu_{\text{eff}} & -\lambda v_d \\ -\frac{g_1 v_d}{\sqrt{2}} & \frac{g_1 v_d}{\sqrt{2}} & -\mu_{\text{eff}} & 0 & -\lambda v_u \\ 0 & 0 & -\lambda v_d & -\lambda v_u & 2\kappa v_s \end{pmatrix}. \quad (16)$$

Chargino sector: The charged higgsinos $\tilde{H}_u^+, \tilde{H}_d^-$ (with mass scale around μ_{eff}) and the charged gaugino \tilde{W}^\pm (with mass scale M_2) can also mix respectively, forming two couples of physical charginos χ_1^\pm, χ_2^\pm .

Gluino sector: As a gauge boson, each gluon also has a same-color superpartner, which is also sorted into gauginos, and whose mass is close to its soft mass M_3 .

Squark and slepton sector: Each quark or charged lepton has two chiral-eigenstate superpartners \tilde{f}_L and \tilde{f}_R , which mix to form two mass-eigenstate superpartners. The mass difference between the two mass eigenstates is proportional to the corresponding trilinear couplings A_f . Since the Yukawa couplings of the first two generations of fermions are very weak, the two superpartners of each fermion can be seen as mass-degenerate. In the NMSSM, with only the left-hand state, each neutrino has only one superpartner, whose mass is equal or close to its soft mass $m_{\tilde{\nu}}$.

scNMSSM: In the fully constrained NMSSM (cNMSSM), like the fully constrained MSSM (cMSSM/mSUGRA), the soft SUSY breaking terms in the Higgs sector are assumed to be unified with those of the squark and slepton sectors at the GUT scale. However, in the semi-constrained NMSSM (scNMSSM), we allow the soft SUSY breaking terms in the Higgs sector to be different. So, in the scNMSSM at the GUT scale,

the universal parameters are [12, 13]:

$$\begin{aligned} M_1 &= M_2 = M_3 \equiv M_{1/2}, \\ M_{\tilde{q}_i}^2 &= M_{\tilde{u}_i}^2 = M_{\tilde{d}_i}^2 = M_{\tilde{l}_i}^2 = M_{\tilde{e}_i}^2 \equiv M_0^2, \\ A_t &= A_b = A_\tau \equiv A_0. \end{aligned} \quad (17)$$

The Higgs soft masses $M_{H_u}^2$, $M_{H_d}^2$ and M_S^2 are allowed to be different from M_0^2 , and the trilinear couplings A_λ , A_κ can be different from A_0 . Since we have three minimisation equations for the VEVs [20], the three Higgs soft masses can be determined with other parameters. Hence, in the scNMSSM we choose the complete parameter sector as:

$$\lambda, \kappa, \tan\beta, \mu_{\text{eff}}, A_\lambda, A_\kappa, A_0, M_0, M_{1/2}. \quad (18)$$

Parameters running in scNMSSM: Parameters at the GUT scale should run via renormalization group equations (RGEs) to SUSY-breaking scale M_{SUSY} . The GUT scale is usually about 10^{16} GeV, and M_{SUSY} is usually chosen to be at 10^3 GeV scale. Then, the approximate running of some parameters can be written as [21, 22]:

$$\begin{aligned} R &\equiv (1 + \tan^2\beta) / (1.29 \tan^2\beta), \\ K &\equiv (1 - R)(A_0 - 2.24 M_{1/2})^2 + 7.84 M_{1/2}^2, \\ A_t &\approx A_0 - R(A_0 - 2.24 M_{1/2}) - 3.97 M_{1/2}, \\ A_b &\approx A_0 - R/6 \cdot (A_0 - 2.24 M_{1/2}) - 3.93 M_{1/2}, \\ M_{\tilde{q}_3}^2 &\approx (1 - R/2) M_0^2 + 7.02 M_{1/2}^2 - K \cdot R/6, \\ M_{\tilde{u}_3}^2 &\approx (1 - R) M_0^2 + 6.6 M_{1/2}^2 - K \cdot R/3, \\ M_{\tilde{d}_3}^2 &\approx M_0^2 + 6.55 M_{1/2}^2, & M_{\tilde{q}_2}^2 &\approx M_0^2 + 7.02 M_{1/2}^2, \\ M_{\tilde{u}_2}^2 &\approx M_0^2 + 6.6 M_{1/2}^2, & M_{\tilde{d}_2}^2 &\approx M_0^2 + 6.55 M_{1/2}^2, \\ A_\tau &\approx A_0 - 0.69 M_{1/2}, & M_{\tilde{l}_3}^2 &\approx M_0^2 + 0.52 M_{1/2}^2, \\ M_{\tilde{e}_3}^2 &\approx M_0^2 + 0.15 M_{1/2}^2, & M_{\tilde{l}_2}^2 &\approx M_0^2 + 0.52 M_{1/2}^2, \\ M_{\tilde{e}_2}^2 &\approx M_0^2 + 0.15 M_{1/2}^2, & M_1 &\approx 0.4 M_{1/2}, \\ M_2 &\approx 0.8 M_{1/2}, & M_3 &\approx 2.4 M_{1/2}. \end{aligned} \quad (19)$$

3 Numerical results and discussion

In this work, we use the program NMSPEC_MCMC [10] in NMSSMTools.5.2.0 [21] to scan the parameter space of the scNMSSM by considering various experimental constraints. We chose the parameter space to scan as follows:

$$0.3 < \lambda < 0.7, \quad 0 < \kappa < 0.7, \quad 1 < \tan\beta < 30,$$

$$100 < \mu_{\text{eff}} < 200 \text{ GeV}, \quad 0 < M_0 < 500 \text{ GeV}, \quad 0 < M_{1/2} < 2 \text{ TeV},$$

$$|A_0| < 10 \text{ TeV}, \quad |A_\lambda| < 10 \text{ TeV}, \quad |A_\kappa| < 10 \text{ TeV}, \quad (20)$$

where we have the following considerations in our choice of parameter space:

1) Small μ_{eff} and M_0 , to get large muon g-2 and also low fine tuning.

2) Large λ (> 0.3) to make our results much different from those of the MSSM in Higgs physics, since there is only one term different in the superpotential between NMSSM and MSSM: $\lambda \hat{S} \hat{H}_u \hat{H}_d$ in Eq. (1), for the doublet-singlet mixing.

3) Smaller $\tan\beta$ (< 30) than in MSSM, as in the NMSSM scenario of h_2 as the 125 GeV SM-like Higgs. In this scenario, we should have $|M_{23}| \ll |M_{33}| < M_{22}$ in the Higgs mass matrix Eq. (12), thus

$$M_A \approx \frac{2\mu}{\sin 2\beta} \approx \mu \tan\beta \approx A_\lambda + \frac{\kappa}{\lambda} \mu. \quad (21)$$

A_λ at the SUSY breaking scale should not be too large, since we have another term of doublet-singlet mixing $\lambda A_\lambda S H_u \cdot H_d$ in the soft breaking terms in Eq. (6).

In the scan, we required the surviving samples to satisfy the following constraints:

1) Theoretical constraints of vacuum stability, and no Landau pole in running λ , κ , and Yukawa couplings below M_{GUT} [10, 21].

2) The second light scalar CP-even Higgs, h_2 , as the SM-like Higgs boson with mass around 125 GeV (e.g., $123 < m_{h_2} < 127$ GeV), with its production rates fitting LHC data globally. For the global fit we used a method like that in our former works [7, 23], with the Higgs data updated with Fig. 3 from Ref. [24] and the left part of Fig. 5 from Ref. [25]. There are 20 experimental data sets in total, so we require $\chi^2 \leq 31.4$, which means each surviving sample fits 20 experimental data sets at 95% confidence level.

3) Constraints of searches for low mass and high mass resonances at LEP, Tevatron, and LHC. These constrain the production rates of light and heavy Higgs. We implemented these constraints by the package `HiggsBounds-5.1.1beta` [26]. We also required the mass of the light Higgs to be $65 \sim 122$ GeV, since we checked that below 65 GeV its diphoton rate is always very small because of the strong constraints at LEP. Also, when the light Higgs is lighter than 62 GeV, exotic decays of the 125 GeV Higgs will be generated, which we have discussed in detail in our former paper [7].

4) Constraints of searches for squarks of the first two generations and gluinos at Run I of the LHC¹⁾. We follow the result in Ref. [13]:

$$m_{\tilde{q}_{1,2}} \gtrsim 900 \text{ GeV}, \quad m_{\tilde{g}} \gtrsim 1400 \text{ GeV}. \quad (22)$$

We use the constraints of mass bounds of chargino and

1) For the stop mass, we checked that our result satisfies the simulation result of $m_{\tilde{t}_1} \gtrsim 500$ GeV in Ref. [27]. For 13 TeV search results at the LHC, all these bounds may be a little higher, but we checked that with stricter constraints, e.g., $m_{\tilde{q}_{1,2}} > 1200$ GeV, $m_{\tilde{g}} > 1800$ GeV, and $m_{\tilde{t}_1} > 600$ GeV, our results, such as muon g-2, do not change much. We will check the exact bounds of these sparticle masses in this model in our future work by doing detailed simulations.

sleptons from LEP. We also checked our surviving samples with SModelS-v1.1.1 [28] (including database v1.1.2 [29])²⁾.

5) Constraints from B physics, such as $B_s \rightarrow \mu^+ \mu^-$, $B_d \rightarrow \mu^+ \mu^-$, $B \rightarrow X_s \gamma$ and $B^+ \rightarrow \tau^+ \nu_\tau$, etc. [36–38].

$$\begin{aligned} 1.7 \times 10^{-9} &< Br(B_s \rightarrow \mu^+ \mu^-) < 4.5 \times 10^{-9}, \\ 1.1 \times 10^{-10} &< Br(B_d \rightarrow \mu^+ \mu^-) < 7.1 \times 10^{-10}, \\ 2.99 \times 10^{-4} &< Br(B \rightarrow X_s \gamma) < 3.87 \times 10^{-4}, \\ 0.70 \times 10^{-4} &< Br(B^+ \rightarrow \tau^+ + \nu_\tau) < 1.58 \times 10^{-4}. \end{aligned} \quad (23)$$

6) Constraints from dark matter relic density from WMAP/Planck [38, 39], the spin-independent (SI) results of direct searches for dark matter at LUX 2017 [40], PandaX-II 2017 [41], and XENON1T 2018 [42], and the spin-dependent (SD) results of direct searches for dark matter by PICO, LUX, and PandaX-II in 2016 [43]. We require the lightest neutralino χ_1^0 to be the dark matter candidate. For the relic density, we only apply the upper bound, e.g., $0 \leq \Omega \leq 0.131$, considering that there may be other sources of dark matter [8, 21].

7) The constraint of the muon anomalous magnetic moment (muon g-2) at 2σ level including the theoretical error. For the experimental data and SM calculation without boson contributions, we use [44, 45]:

$$a_\mu^{\text{ex}} = (11659208.0 \pm 6.3) \times 10^{-10}, \quad (24)$$

$$\delta a_\mu \equiv a_\mu^{\text{ex}} - a_\mu^{\text{SM}} = (27.4 \pm 9.3) \times 10^{-10} \quad (25)$$

We calculate the SUSY contribution δa_μ including SM-like bosons, and require it to satisfy δa_μ at 2σ level. We also include our error in the SUSY δa_μ calculation, which is about 1.5×10^{-10} .

8) The theoretical constraint of low fine tuning from the GUT scale, which is defined by [46]:

$$FT = \text{Max} \left\{ \left| \frac{\partial \ln(M_Z)}{\partial \ln(p_i^{\text{GUT}})} \right| \right\}, \quad (26)$$

where each p_i^{GUT} denotes a parameter at the GUT scale:

$$p_i^{\text{GUT}} = M_{\tilde{H}_u}, M_{\tilde{H}_d}, M_{\tilde{S}}, M_0, M_{1/2}, A_\lambda, A_\kappa, A_0, \lambda, \kappa, y_t, g, M_{\text{GUT}}, \quad (27)$$

where $g = \sqrt{g_1^2 + g_2^2}/2$, y_t is the Yukawa coupling of the top quark, and M_{GUT} is the GUT scale. We require $FT < 1000$ for each surviving sample.

We take a modified multi-path Markov Chain Monte Carlo (MCMC) scan in parameter space, where we do not use likelihood functions. Instead we require each good point to satisfy all our experimental constraints at 2σ level, or below the upper limits of 95% (for the DM direct detection, it is 90% following data released by the

collaborations). Each time we get a good point surviving all our constraints, we save the point, and search for the next good point around the former one. Since we use a Gaussian random number and set a not-small standard step, the later good point can be much different from the former one, which ensures we get as much as possible of the surviving parameter space available. In total, we get nearly 10^6 surviving samples. As some samples may be very similar to each other, we remove most repetitive samples by calculating the distance between them. First, we normalize all samples by using min-max normalization (MMN), which is just a linear transformation of the original data. We normalize each sample to 9 dimensions, as there are 9 free parameters x^i in the scan

$$\hat{x}^i = \frac{x^i - x_{\min}^i}{x_{\max}^i - x_{\min}^i} \quad (i=1, \dots, 9) \quad (28)$$

After this linear transformation, all of these 9 new parameters \hat{x}^i will fall in $[0, 1]$. Then we calculate the Euclidean distance between all these surviving samples. If the distance between two points is too small, we just select one of them randomly. For each panel in the following figures, to make them look good and be of small size, we take a MMN similarly but in 3 dimensions, which are the horizontal, vertical and color-indicated quantities.

In Fig. 1, we project the surviving samples on the $\lambda - \tan\beta$, $A_0 - M_{1/2}$ and $A_0 - M_0$ planes. We show fine tuning from the GUT scale (left and middle panels) and the lighter stop mass $m_{\tilde{t}_1}$ (right panel) by different colors. We can see from the left and middle panels that fine tuning FT can be as low as around 150 at most. In the left panel, we can also see that low-fine-tuning samples are mostly located in the $\tan\beta \lesssim 15$, or $15 \lesssim \tan\beta \lesssim 25$ but $\lambda \lesssim 0.4$ regions. This is because, according to the minimisation equation of v_u [46],

$$M_{H_u}^2 + \mu^2 + \frac{1}{2} X m_Z^2 = 0, \quad (29)$$

where

$$\begin{aligned} X = & \frac{\tan^2\beta - 1}{\tan^2\beta + 1} + \frac{\tan^2\beta}{\tan^2\beta + 1} \frac{3y_t^4}{8\pi^2 g^2} \ln \frac{m_{\tilde{t}}^2}{m_t^2} \\ & - \frac{1}{\tan\beta} \left(\frac{\mu A_\lambda}{m_Z^2} + \frac{\kappa \mu^2}{\lambda m_Z^2} \right) + \frac{\lambda^2}{g^2} \frac{2}{\tan^2\beta + 1} \end{aligned} \quad (30)$$

is a function of $\lambda, \tan\beta$, etc. We checked that for most of the surviving samples, the largest fine tuning comes from parameter M_{H_u} , and that of the rest comes from parameter λ . According to RGE running, $|M_{H_u}^2|$ is related to $M_0, M_{1/2}$, and A_0 , thus we can see from the middle panel that samples with small $M_{1/2}$ and A_0 usually

2) This includes many constraints on stop \tilde{t}_1 [30–33], chargino χ_1^\pm and neutralino χ_2^0 [34, 35]. We checked that it cannot give the surviving samples further strong constraints, because for the surviving samples: χ_1^\pm are Higgsino-like, and $\chi_{1,2}^0$ are Higgsino or singlino-like, thus light χ_1^\pm and χ_2^0 mainly decay to χ_1^0 and a pair of quarks, each channel with about 10–20 percent; most charginos and neutralinos are lighter than \tilde{t}_1 . Thus \tilde{t}_1 can have many decay channels, where even the dominant channel, e.g., $\tilde{t}_1 \rightarrow b\chi_1^+$, cannot be over half.

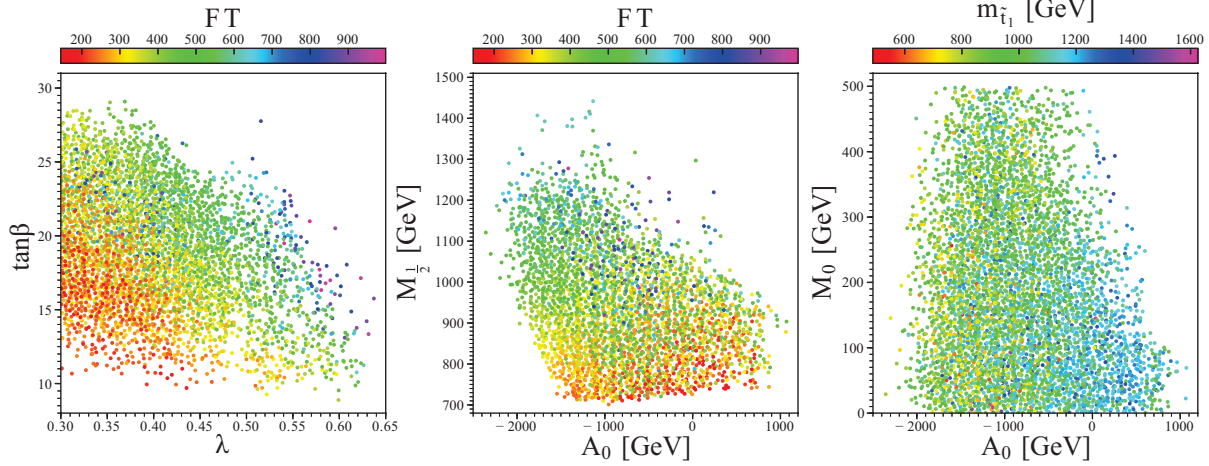


Fig. 1. (color online) Surviving samples in the $\tan\beta$ versus λ (left), $M_{1/2}$ versus A_0 (middle), and M_0 versus A_0 (right) planes. Colors in the left and middle panels indicate fine tuning from GUT scale, while colors in the right panel indicate the mass of the lighter stop \tilde{t}_1 .

have low fine tuning. From the middle and right panels, we can see that these surviving regions are not symmetric around $A_0 = 0$, where negative A_0 is more favored. This is because at SUSY-breaking scale we have $M_{43}^2 \approx M_0^2 + 6.55M_{1/2}^2$ and

$$A_t \approx A_0 - \frac{(A_0 - 2.24M_{1/2})(1 + \tan^2\beta)}{(1.29\tan^2\beta)} - 3.97M_{1/2} \approx 0.22(A_0 - 10M_{1/2}) \quad (31)$$

according to the RGEs. We have $M_{1/2} \gtrsim 700$ GeV, mainly because we require $m_{\tilde{g}} \gtrsim 1400$ GeV, while at SUSY-breaking scale $M_3 \approx 2.4M_{1/2}$. Later we can see from Fig. 4 that $M_{1/2}$ has upper bounds of about 1500 GeV mainly because of the constraint of muon $g-2$. Finally, in the right panel, we can see the mass of the stop can be as low as about 500 GeV. We will continue studying these light-stop cases in our future work, by doing detailed simulations based on the search results at the 13 TeV LHC.

In Fig. 2, we project the surviving samples on the λ versus κ (left), and $R(pp \rightarrow h_1 \rightarrow \gamma\gamma)$ versus m_{h_1} (middle and right) planes respectively. We show the singlet component in h_1 (left and middle panels) and the reduced squared coupling $|C_{h_1\gamma\gamma}/SM|^2$ (right panel) by different colors. We can see from the left and middle panels that most of the samples have $|S_{13}|^2$ approaching 1, which means they are highly singlet-dominated. The singlet component in h_1 is 0.5 at least, since h_2 is the SM-like Higgs. It can be sorted into two regions in the λ - κ plane:

$$\begin{aligned} \lambda \gtrsim 1.5\kappa \text{ region, where } h_1 \text{ are highly-singlet-dominated} \\ (|S_{13}|^2 \gtrsim 0.8) \\ \lambda \lesssim 1.5\kappa \text{ region, including smaller-} |S_{13}|^2 \text{ samples} \\ (0.5 \lesssim |S_{13}|^2 \lesssim 0.8) \end{aligned} \quad (32)$$

The samples of $|S_{13}|^2 \lesssim 0.9$ are mainly in the latter region, because in the former region, with small κ/λ we will have $|M_{23}^2| \ll |M_{22}^2|$, which will result in very little mixing between singlet and SM-like doublet, thus very little singlet component in h_2 and very little doublet component in h_1 . From the middle panel, we find that doublet-singlet mixing can only be considerable ($|S_{13}|^2 \lesssim 0.9$) when $m_{h_1} \gtrsim 90$ GeV. Combining the middle and right panels we can also see that some highly-singlet-dominated h_1 samples ($|S_{13}|^2 \gtrsim 0.8$) can provide a considerable diphoton rate $R(pp \rightarrow h_1 \rightarrow \gamma\gamma)$, while the rates are not so large for smaller- $|S_{13}|^2$ samples ($0.5 \lesssim |S_{13}|^2 \lesssim 0.8$). This is because for the former samples, we have light higgsino-like chargino (see Fig. 4) and moderate λ , thus large $h_1\gamma\gamma$ loop-reduced coupling and large $h_1 \rightarrow \gamma\gamma$ branching ratio. For the latter samples, the h_1 reduced coupling to $\gamma\gamma$ can be smaller than to other SM particles like $b\bar{b}$, thus the $h_1 \rightarrow \gamma\gamma$ branching ratio cannot be large. We checked that the reduced $h_1\gamma\gamma$ coupling can be two times that of the doublet component in h_1 ($1 - |S_{13}|^2$) for the former, while it can only be about 0.5 for the latter. According to the latest result of the search for low-mass resonances by CMS, the suspected resonance is at around 95 GeV, with a diphoton rate of about 0.5 ± 0.2 [5]. We can see that we have some samples providing such a signal. In Table 1, we provide the detailed information of four such samples for further study. The search results for low-mass resonances by ATLAS at Run I of the LHC [47] are also shown on the middle and right panels. We can see that the upper limit from ATLAS is higher than that from CMS, and further results from ATLAS are needed to cross check the suspected excess.

In Fig. 3 we show the properties of dark matter in the scNMSSM. In this work, we require the lightest neutralino χ_1^0 to be the LSP and to constitute dark matter by

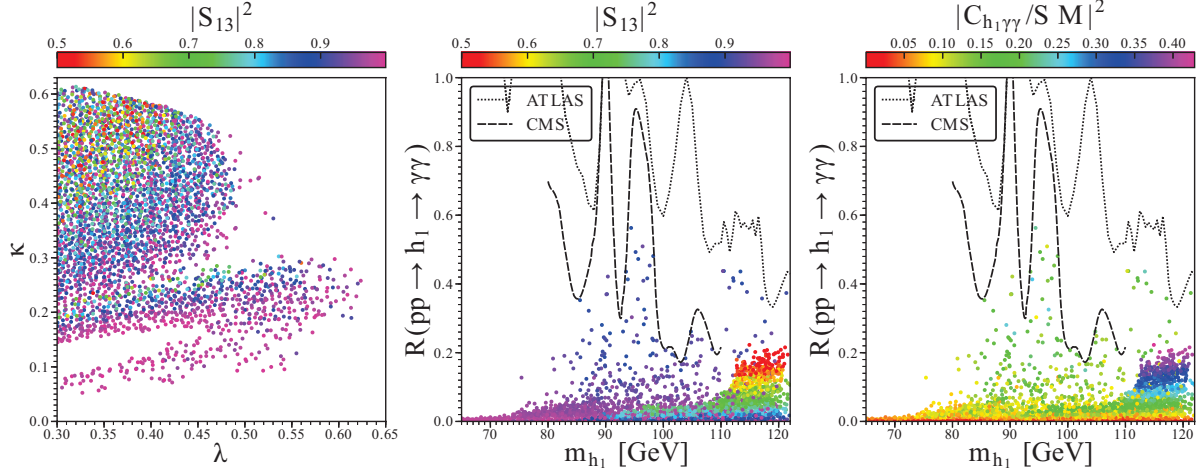


Fig. 2. (color online) Surviving samples in the κ versus λ (left), and diphoton production rate of the lightest Higgs h_1 versus its mass m_{h_1} (middle and right) planes. In the middle and right panels, the black dotted and dashed line indicates the observed exclusion limits (95% CL) from ATLAS [47] and CMS [5] on $R(pp \rightarrow h_1 \rightarrow \gamma\gamma)$ respectively. Colors in the left and middle panels indicate the singlet component in h_1 , while colors in the right panel indicate the squared effective coupling of h_1 with two photons, reduced by its corresponding SM value, i.e. $|C_{h_1\gamma\gamma}/SM|^2$.

Table 1. Four representative samples predicting the diphoton rate hinted at by CMS data, where $R_{h_1 \rightarrow \gamma\gamma}$ is the same as $R(gg \rightarrow h_1 \rightarrow \gamma\gamma)$ elsewhere in this paper.

	λ	κ	$\tan\beta$	$\mu_{\text{eff}}/\text{GeV}$	$A_\lambda^{\text{GUT}}/\text{GeV}$	$A_\kappa^{\text{GUT}}/\text{GeV}$	A_0/GeV	M_0/GeV	$M_{1/2}/\text{GeV}$	m_{h_1}/GeV	$R_{h_1 \rightarrow \gamma\gamma}$
P1	0.51	0.26	20.2	130.3	3856.1	2707.1	-172.6	23.3	894.3	96.7	0.33
P2	0.42	0.22	16.1	145.5	2271.8	953.5	-997.1	163.3	754.0	95.6	0.47
P3	0.31	0.18	21.4	165.8	2923.6	439.1	-1084.2	10.8	1006.2	96.4	0.51
P4	0.37	0.20	18.7	137.8	2363.8	700.0	-826.6	97.5	827.9	95.2	0.49

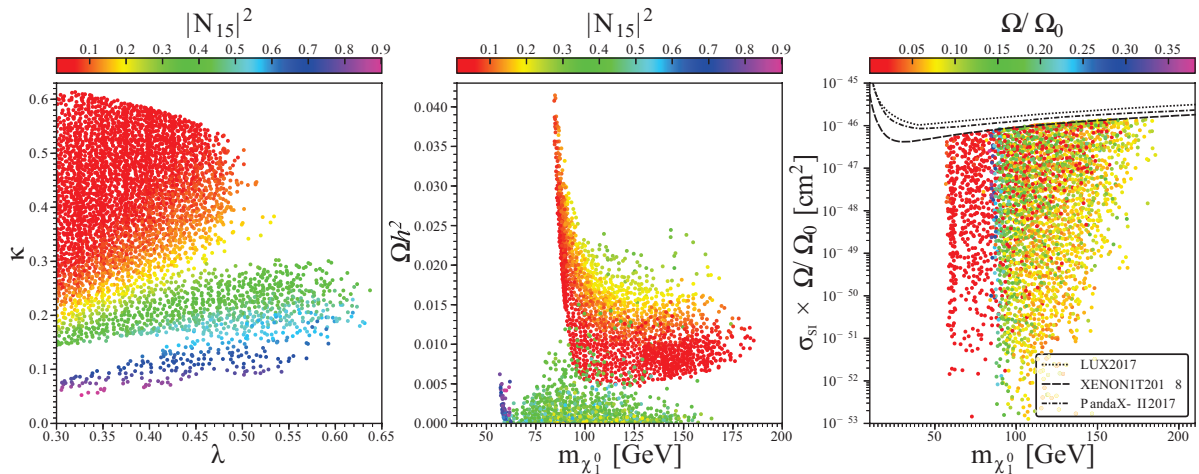


Fig. 3. Surviving samples in the κ versus λ (left), dark matter relic density Ωh^2 versus the lightest neutralino (LSP) mass $m_{\chi_1^0}$ (middle), and spin-independent dark matter and nucleon scattering cross section ($\sigma_{\text{SI}} \times \Omega/\Omega_0$) versus LSP mass $m_{\chi_1^0}$ (right) planes. In the middle and right panels, the black dotted, dot-dashed, and dashed lines indicate the observed exclusion limits (90% CL) on $\sigma_{\text{SI}} \times \Omega/\Omega_0$ released by LUX 2017, PandaX-II 2017 and XENON1T 2018, respectively. Colors in the left and middle panels indicate the singlino component in χ_1^0 , while colors in the right panel indicate the ratio of LSP relic density in the observed value (Ω/Ω_0), where $\Omega_0 h^2 = 0.1187$ [38, 39].

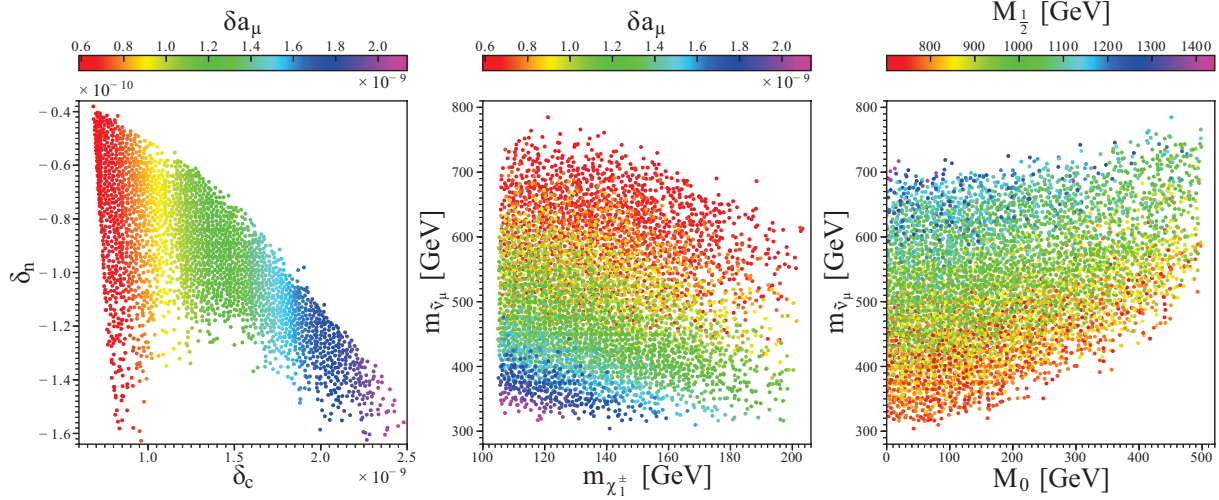


Fig. 4. (color online) Surviving samples in the neutralino-smuon contribution δ_n versus chargino-sneutrino contribution δ_c to muon g-2 (left), light chargino mass $m_{\chi_1^\pm}$ versus muon sneutrino mass $m_{\tilde{\nu}_\mu}$ (middle), and $m_{\tilde{\nu}_\mu}$ versus parameter M_0 (right) planes. Colors in the left and middle panels indicate muon g-2 (δa_μ), while colors in the right panel indicate parameter $M_{1/2}$.

a ratio of Ω/Ω_0 , with the right relic density $\Omega_0 h^2 = 0.1187$ [38, 39]. Hence we adjust the SI scattering cross section of each sample by tuning the corresponding ratio Ω/Ω_0 . Since the results of searches for gluinos at the LHC require $M_3 \simeq m_{\tilde{g}} \gtrsim 1400$ GeV, and the universal gaugino mass at GUT scale requires

$$M_1 : M_2 : M_3 \approx 1 : 2 : 6, \quad (33)$$

while $\mu_{\text{eff}} < 200$ GeV and $\kappa v_S = \mu_{\text{eff}} \kappa / \lambda$, according to the tree-level neutralino mass matrix Eq.(16), we can infer that the main components of χ_1^0 can only be the singlino and higgsino. From the left panel of Fig.3, we can see clearly that

$$\begin{aligned} \text{when } \lambda \gtrsim 1.5\kappa: |N_{15}|^2 \gtrsim 0.3, \chi_1^0 \text{ is singlino-dominated} \\ \text{when } \lambda \lesssim 1.5\kappa: |N_{15}|^2 \lesssim 0.3, \chi_1^0 \text{ is Higgsino-dominated.} \end{aligned} \quad (34)$$

We can categorize the surviving samples into three classes, which can be called the h/Z funnel, focus point, and A_1 funnel scenarios respectively, as in Ref. [48].

1) From the middle and right panels of Fig. 3, we can see that in the h/Z funnel scenario, its mass $m_{\chi_1^0} \lesssim m_{h_2}/2$, and its relic density is only about 1/10 of the WMAP data at most. For some samples the SI scattering cross section before adjustment with Ω/Ω_0 are above the exclusion limit by XENON1T 2018, LUX 2017, and PandaX-II 2017. Combining with the left panel, we can see that, in the h/Z funnel scenario, the larger λ the smaller its relic density. This is because a pair of singlet-dominated χ_1^0 annihilates to a pair of SM particles through the SM-like Higgs h_2 , and the coupling

$h_2 \chi_1^0 \chi_1^0$ is proportional to λ :

$$\begin{aligned} C_{h_2 \chi_1^0 \chi_1^0} &= \sqrt{2} \lambda N_{15} [S_{21} (N_{14} \cos \beta - N_{13} \sin \beta) \\ &\quad + S_{22} (N_{14} \sin \beta + N_{13} \cos \beta)] - \sqrt{2} \kappa S_{23} |N_{15}|^2 \\ &\quad + (g_2 N_{12} - g_1 N_{11}) [S_{21} (N_{13} \cos \beta + N_{14} \sin \beta) \\ &\quad + S_{22} (N_{13} \sin \beta - N_{14} \cos \beta)] \\ &\approx \sqrt{2} \lambda S_{22} N_{15} (N_{14} \sin \beta + N_{13} \cos \beta) \\ &\quad - \sqrt{2} \kappa S_{23} |N_{15}|^2, \end{aligned} \quad (35)$$

since $|S_{22}| \gg |S_{23}| \gg |S_{21}|$, $|N_{15}| \gg |N_{13,14}| \gg |N_{11,12}|$, and $\lambda > \kappa$. Besides, the SI scattering of χ_1^0 with SM particles is also mainly mediated by the SM-like h_2 . Thus, we can infer that, with smaller λ , the relic density of χ_1^0 can be larger, and the SI scattering cross section can be smaller. Of course, to have χ_1^0 singlino-dominated, we also need even smaller κ .

2) In the focus point scenario, when $m_{\chi_1^0}$ is slightly larger than m_W , the main annihilation mechanism is $\chi_1^0 \chi_1^0 \rightarrow W^+ W^-$ though the t or u channel chargino, or s channel Z or scalars. A peak of relic density appears around $m_{\chi_1^0} \approx m_W$ in the middle panel of Fig. 3, because the relic density is inversely proportional to $\sqrt{1 - m_W^2/m_{\chi_1^0}^2}$ [49]. The relic density cannot be even larger, because it is very hard for a higgsino-like χ_1^0 to unlimitedly approximate to m_W , and also the results for SI scattering cross section in 2018 give even stronger constraints on this scenario.

3) For the other samples, including both singlet-dominated and higgsino-dominated χ_1^0 cases, the main annihilation mechanism is the A_1 funnel, where the light CP-odd scalar A_1 is usually singlet-dominated ($\gtrsim 90\%$), but has a φ_d composition of several percent. Thus there

can be a large $A_1\chi_1^0\chi_1^0$ coupling for large λ or κ , and a considerable $A_1b\bar{b}$ coupling for the φ_d composition and large $\tan\beta$. In this scenario, a pair of χ_1^0 mainly annihilates through A_1 , and $b\bar{b}$ and $\tau^+\tau^-$ are produced.

We also consider the spin-dependent (SD) results of direct detection for dark matter [43]. However, we checked that the current upper exclusion limits of SD results are much higher than the SI ones, and they impose no further constraints on our surviving samples. So in this work, we do not discuss the SD results further.

From the left panel of Fig. 4, we can interpret muon g-2 (δa_μ) at 1σ level, and the main contribution comes from the loop of chargino χ_1^\pm and muon sneutrino $\tilde{\nu}_\mu$. The loop of the lightest neutralino χ_1^0 and smuon $\tilde{\mu}_i$ cannot contribute as much as in the MSSM, because χ_1^0 is singlino-dominated or higgsino-dominated, neither of which has a strong enough coupling with the muon and its partner. From the middle panel of Fig. 4 we can see that the chargino loop can contribute much because both the chargino χ_1^0 and muon sneutrino $\tilde{\nu}_\mu$ can be very light. The lighter they are, the larger muon g-2 is. From the right panel, the sneutrino mass is mainly determined by M_0 and $M_{1/2}$. In fact, the relation is roughly $m_{\tilde{\nu}_\mu} \approx \sqrt{M_0^2 + 0.52M_{1/2}^2}$. Combined with $M_3 \approx 2.4M_{1/2}$, we can infer and have checked that, with higher gluino mass $m_{\tilde{g}} \approx 2$ TeV, the sneutrino mass can still be low as about 400 GeV, and thus muon g-2 can still satisfy the data at 1σ level.

4 Conclusions

In this work, we have checked the status of the scNMSSM under current constraints, such as 125 GeV Higgs data, searches for low and high mass resonances, searches for SUSY particles at the LHC, B physics, muon g-2, dark matter relic density by WMAP/Planck, and direct searches for dark matter by LUX 2017, PandaX-II 2017, and XENON1T 2018. First, we scanned the parameter space of the scNMSSM in 9 dimensions with the MCMC method. For each valid sample, we calculated its vari-

ous physical quantities and required them to satisfy corresponding constraints. For the surviving samples, we analyzed fine tuning from the GUT scale, SUSY particle masses, the light scalar and its diphoton signal, dark matter relic density and direct detection, muon g-2, and their favoured parameter space. Finally, we come to the following conclusions regarding the scNMSSM:

1) For low fine tuning samples, small μ_{eff} , M_0 , $M_{1/2}$, A_0 , are more favored, and the lighter stop mass can be as low as about 500 GeV, which can be further checked in future works with search results at the 13 TeV LHC.

2) For light higgsino-like charginos and moderate λ , the highly-singlet-dominated light scalar can have a considerable diphoton rate, satisfying the latest results of the search for low-mass resonances by CMS.

3) For high gluino bounds at the LHC and the condition of universal gauginos at the GUT scale, the lightest neutralino can only be singlino-dominated or higgsino-dominated. Their mass regions are $m_{\chi_1^0} \lesssim m_W$ and $m_W \lesssim m_{\chi_1^0} \lesssim 200$ GeV, and annihilation scenarios are mainly h/Z funnel and focus point respectively. The results for SI scattering cross section in 2017/2018 give strong constraints, especially for the focus point scenario.

4) For light muon sneutrino and light higgsino-like charginos, we can get large muon g-2, while the contribution of neutralinos cannot be large because bino-like and wino-like neutralinos are heavy.

5) The model can satisfy all the above constraints, although it is not easy for the lightest neutralino, as the only dark matter candidate, to get enough relic density.

Considering the disadvantage of the scNMSSM, one can try three main kinds of ways to raise the relic density:

1) Considering other source of relic density, e.g., the effects of modifications of the expansion rate and of the entropy content in the early universe.

2) Changing the LSP to another sparticle, such as bino-like neutralinos in the non-universal gaugino cases, or sneutrinos in the right-handed neutrinos extended case.

3) Reducing λ and κ in the h/Z funnel scenario, although this way may lose a light Higgs.

References

- 1 G. Aad et al (ATLAS Collaboration), Phys. Lett. B, **716**: 1 (2012)
- 2 S. Chatrchyan et al (CMS Collaboration), Phys. Lett. B, **716**: 30 (2012)
- 3 J. Cao, Z. Heng, D. Li, and J. M. Yang, Phys. Lett. B, **710**: 665 (2012), arXiv: 1112.4391 [hep-ph]; C. Han, K. i. Hikasa, L. Wu, J. M. Yang, and Y. Zhang, Phys. Lett. B, **769**: 470 (2017), arXiv: 1612.02296 [hep-ph]
- 4 J. Cao, Z. Heng, J. M. Yang, and J. Zhu, JHEP, **1210**: 079 (2012), arXiv: 1207.3698 [hep-ph]; J. J. Cao, Z. X. Heng, J. M. Yang, Y. M. Zhang, and J. Y. Zhu, JHEP, **1203**: 086 (2012), arXiv: 1202.5821 [hep-ph]
- 5 CMS Collaboration (CMS Collaboration), CMS-HIG-17-013, arXiv:1811.08459 [hep-ex]
- 6 G. Brooijmans et al, arXiv:1803.10379 [hep-ph]; J. H. Kim and I. M. Lewis, arXiv:1803.06351 [hep-ph]; N. Bizot, G. Cacciapaglia and T. Flacke, arXiv:1803.00021 [hep-ph]; U. Haisch, J. F. Kamenik, A. Malinauskas, and M. Spira, JHEP, **1803**: 178 (2018), arXiv: 1802.02156 [hep-ph]; X. F. Han and L. Wang, arXiv:1801.08317 [hep-ph]; U. Haisch and A. Malinauskas, JHEP, **1803**: 135 (2018), arXiv: 1712.06599 [hep-ph]; F. Richard, arXiv:1712.06410 [hep-ex]; G. F. Giudice, Y. Kats, M. McCullough, R. Torre, and A. Urbano, arXiv:1711.08437 [hep-ph]; R. Vega, R. Vega-Morales, and K. Xie, JHEP, **1803**: 168 (2018), arXiv: 1711.05329 [hep-ph]; G. Caccia-

- paglia, G. Ferretti, T. Flacke, and H. Serodio, arXiv:1710.11142 [hep-ph]; A. Crivellin, J. Heeck and D. Mller, Phys. Rev. D, **97**(3): 035008 (2018), arXiv: 1710.04663 [hep-ph]; A. Mariotti, D. Redigolo, F. Sala, and K. Tobioka, arXiv:1710.01743 [hep-ph]; D. Liu, J. Liu, C. E. M. Wagner and X. P. Wang, JHEP **1806**, 150 (2018) arXiv:1805.01476 [hep-ph]; J. Q. Tao *et al.*, Chin. Phys. C **42**, no. 10, 103107 (2018) arXiv:1805.11438 [hep-ph]; F. Domingo, S. Heinemeyer, S. Paehr and G. Weiglein, arXiv:1807.06322 [hep-ph]; T. Biekter, S. Heinemeyer and C. Muoz, Eur. Phys. J. C **78** (2018) no.6, 504 arXiv:1712.07475 [hep-ph]
- 7 J. Cao, F. Ding, C. Han, J. M. Yang, and J. Zhu, JHEP, **1311**: 018 (2013), arXiv: 1309.4939 [hep-ph]; C. T. Potter, Eur. Phys. J. C, **76**(1): 44 (2016), arXiv: 1505.05554 [hep-ph]; F. Mahmoudi, J. Rathman, O. Stal, and L. Zeune, Eur. Phys. J. C, **71**: 1608 (2011), arXiv: 1012.4490 [hep-ph]; F. Domingo, JHEP, **1703**: 052 (2017), arXiv: 1612.06538 [hep-ph]; M. Badziak and C. E. M. Wagner, JHEP, **1702**: 050 (2017), arXiv: 1611.02353 [hep-ph]; E. Conte, B. Fuks, J. Guo, J. Li, and A. G. Williams, JHEP, **1605**: 100 (2016), arXiv: 1604.05394 [hep-ph]; U. Ellwanger and M. Rodriguez-Vazquez, JHEP, **1602**: 096 (2016), arXiv: 1512.04281 [hep-ph]; R. Benbrik, M. Gomez Bock, S. Heinemeyer, O. Stal, G. Weiglein and L. Zeune, Eur. Phys. J. C **72** (2012) 2171 arXiv:1207.1096 [hep-ph]
 - 8 J. Cao, X. Guo, Y. He, P. Wu, and Y. Zhang, Phys. Rev. D, **95**(11): 116001 (2017), arXiv: 1612.08522 [hep-ph]
 - 9 K. Kowalska, S. Munir, L. Roszkowski, E. M. Sessolo, S. Trojanowski, and Y. L. S. Tsai, Phys. Rev. D, **87**: 115010 (2013), arXiv: 1211.1693 [hep-ph]; J. F. Gunion, Y. Jiang, and S. Kraml, Phys. Lett. B, **710**: 454 (2012), arXiv: 1201.0982 [hep-ph]
 - 10 U. Ellwanger and C. Hugonie, Comput. Phys. Commun., **177**: 399 (2007), [hep-ph/0612134]
 - 11 U. Ellwanger, A. Florent, and D. Zerwas, JHEP, **1101**: 103 (2011), arXiv: 1011.0931 [hep-ph]; G. Panotopoulos, J. Phys. Conf. Ser., **259**: 012064 (2010), arXiv: 1010.4481 [hep-ph]; D. E. Lopez-Fogliani, L. Roszkowski, R. Ruiz de Austri, and T. A. Varley, Phys. Rev. D, **80**: 095013 (2009), arXiv: 0906.4911 [hep-ph]; G. Belanger, C. Hugonie, and A. Pukhov, JCAP, **0901**: 023 (2009), arXiv: 0811.3224 [hep-ph]; A. Djouadi, U. Ellwanger, and A. M. Teixeira, JHEP, **0904**: 031 (2009), arXiv: 0811.2699 [hep-ph]; U. Ellwanger, AIP Conf. Proc., **1078**: 73 (2009), arXiv: 0809.0779 [hep-ph]; C. Hugonie, G. Belanger, and A. Pukhov, JCAP, **0711**: 009 (2007), arXiv: 0707.0628 [hep-ph]
 - 12 D. Das, U. Ellwanger, and A. M. Teixeira, JHEP, **1304**: 117 (2013), arXiv: 1301.7584 [hep-ph]
 - 13 U. Ellwanger and C. Hugonie, JHEP, **1408**: 046 (2014), arXiv: 1405.6647 [hep-ph]
 - 14 D. G. Cerdeno, V. De Romeri, V. Martin-Lozano, K. A. Olive, and O. Seto, Eur. Phys. J. C, **78**(4): 290 (2018), arXiv: 1707.03990 [hep-ph]
 - 15 A. Arbey and F. Mahmoudi, JHEP, **1005**: 051 (2010), arXiv: 0906.0368 [hep-ph]
A. Arbey and F. Mahmoudi, Phys. Lett. B, **669**: 46 (2008), arXiv: 0803.0741 [hep-ph]
 - 16 U. Ellwanger, C. Hugonie, and A. M. Teixeira, Phys. Rept., **496**: 1 (2010); M. Maniatis, Int. J. Mod. Phys. A, **25**: 3505 (2010),
 - 17 S. P. Martin, Adv. Ser. Direct. High Energy Phys., **21**: 1 (2010); Adv. Ser. Direct. High Energy Phys., **18**: 1 (1998), [hep-ph/9709356]
 - 18 D. J. Miller, R. Nevzorov, and P. M. Zerwas, Nucl. Phys. B, **681**: 3 (2004) [hep-ph/0304049]
 - 19 U. Ellwanger, J. F. Gunion, and C. Hugonie, JHEP, **0502**: 066 (2005); U. Ellwanger and C. Hugonie, Comput. Phys. Commun., **175**: 290 (2006)
 - 20 U. Ellwanger, C. Hugonie, and A. M. Teixeira, Phys. Rept., **496**: 1 (2010), arXiv: 0910.1785 [hep-ph]
 - 21 U. Ellwanger, J. F. Gunion, and C. Hugonie, JHEP, **0502**: 066 (2005), [hep-ph/0406215]
U. Ellwanger and C. Hugonie, Comput. Phys. Commun., **175**: 290 (2006), [hep-ph/0508022]
 - 22 U. Ellwanger, C.-C. Jean-Louis, and A. M. Teixeira, JHEP, **0805**: 044 (2008), arXiv: 0803.2962 [hep-ph]
 - 23 J. Cao, Y. He, P. Wu, M. Zhang, and J. Zhu, JHEP, **1401**: 150 (2014), doi:10.1007/JHEP01(2014)150, arXiv: 1311.6661 [hep-ph]
 - 24 The ATLAS collaboration (ATLAS Collaboration), ATLAS-CONF-2015-007
 - 25 V. Khachatryan et al (CMS Collaboration), Eur. Phys. J. C, **75**(5): 212 (2015), doi:10.1140/epjc/s10052-015-3351-7, arXiv: 1412.8662 [hep-ex]
 - 26 P. Bechtle, O. Brein, S. Heinemeyer, O. Stal, T. Stefaniak, G. Weiglein, and K. E. Williams, Eur. Phys. J. C, **74**(3): 2693 (2014), arXiv: 1311.0055 [hep-ph]
 - 27 J. Cao, Y. He, L. Shang, W. Su, and Y. Zhang, JHEP, **1608**: 037 (2016), arXiv: 1606.04416 [hep-ph]
 - 28 F. Ambrogio et al, Comput. Phys. Commun., **227**: 72 (2018), arXiv: 1701.06586 [hep-ph]
 - 29 S. Kraml, S. Kulkarni, U. Laa, A. Lessa, W. Magerl, D. Proschofsky-Spindler, and W. Waltenberger, Eur. Phys. J. C, **74**: 2868 (2014), arXiv: 1312.4175 [hep-ph]
 - 29 <http://smodels.hephy.at/wiki/ListOfAnalysesv112WithSuperseded>
 - 30 A. M. Sirunyan et al (CMS Collaboration), Phys. Rev. D, **96**(3): 032003 (2017), arXiv: 1704.07781 [hep-ex]
 - 31 A. M. Sirunyan et al (CMS Collaboration), Eur. Phys. J. C, **77**(10): 710 (2017), arXiv: 1705.04650 [hep-ex]
 - 32 A. M. Sirunyan et al (CMS Collaboration), Phys. Rev. D, **97**(3): 032009 (2018) arXiv: 1711.00752 [hep-ex]
 - 33 A. M. Sirunyan et al (CMS Collaboration), JHEP, **1710**: 019 (2017) arXiv: 1706.04402 [hep-ex]
 - 34 A. M. Sirunyan et al (CMS Collaboration), JHEP, **1711**: 029 (2017) arXiv: 1706.09933 [hep-ex]
 - 35 A. M. Sirunyan et al (CMS Collaboration), JHEP, **1803**: 160 (2018) arXiv: 1801.03957 [hep-ex]
 - 36 [BaBar Collaboration], Phys. Rev. Lett., **109**: 191801 (2012); Phys. Rev. Lett., **109**: 101802 (2012)
 - 37 (LHCb Collaboration), Phys. Rev. Lett., **110**: 021801 (2013)
 - 38 C. Patrignani et al (Particle Data Group), Chin. Phys. C, **40**(10): 100001 (2016)
 - 39 P. A. R. Ade et al (Planck Collaboration), Astron. Astrophys., **571**: A16 (2014), arXiv: 1303.5076 [astro-ph.CO]
G. Hinshaw et al (WMAP Collaboration), Astrophys. J. Suppl., **208**: 19 (2013) arXiv: 1212.5226 [astro-ph.CO]
 - 40 D. S. Akerib et al (LUX Collaboration), Phys. Rev. Lett., **118**(2): 021303 (2017), arXiv: 1608.07648 [astro-ph.CO]
 - 41 X. Cui et al (PandaX-II Collaboration), Phys. Rev. Lett., **119**(18): 181302 (2017), arXiv: 1708.06917 [astro-ph.CO]
 - 42 E. Aprile et al (XENON Collaboration), arXiv:1805.12562 [astro-ph.CO]
 - 43 C. Amole et al (PICO Collaboration), Phys. Rev. D, **93**(6): 061101 (2016), arXiv: 1601.03729 [astro-ph.CO]
D. S. Akerib et al (LUX Collaboration), Phys. Rev. Lett., **116**(16): 161302 (2016) arXiv: 1602.03489 [hep-ex]
C. Fu et al (PandaX-II Collaboration), Phys. Rev. Lett., **118**(7): 071301 (2017); Phys. Rev. Lett., **120**(4): 049902 (2018), arXiv: 1611.06553 [hep-ex]
 - 44 G. W. Bennett et al (Muon g-2 Collaboration), Phys. Rev. D, **73**: 072003 (2006), [hep-ex/0602035]
 - 45 F. Jegerlehner, Acta Phys. Polon. B, **38**: 3021 (2007), [hep-ph/0703125] J. Bijnens and J. Prades, Mod. Phys. Lett. A, **22**: 767 (2007), [hep-ph/0702170 [HEP-PH] S. Heinemeyer, D. Stockinger, and G. Weiglein, Nucl. Phys. B, **699**: 103 (2004), [hep-ph/0405255] A. Czarniecki, W. J. Marciano, and

- A. Vainshtein, Phys. Rev. D, **67**: 073006 (2003); Phys. Rev. D, **73**: 119901 (2006), [hep-ph/0212229]
- 46 U. Ellwanger, G. Espitalier-Noel, and C. Hugonie, JHEP, **1109**: 105 (2011), arXiv: 1107.2472 [hep-ph]
- 47 G. Aad et al (ATLAS Collaboration), Phys. Rev. Lett., **113**(17): 171801 (2014), arXiv: 1407.6583 [hep-ex]
- 48 E. A. Bagnaschi et al, Eur. Phys. J. C, **75**: 500 (2015), arXiv: 1508.01173 [hep-ph]
- 49 G. Jungman, M. Kamionkowski, and K. Griest, Phys. Rept., **267**: 195 (1996), [hep-ph/9506380]